Scientific Research Publishing

Advances in Microbiology, 2024, 14, 137-161
https://www.scirp.org/journal/aim
ISSN Online: 2165-3410
ISSN Print: 2165-3402

Bioremediation of Textile Azo Dyes Amido Black 10B, Reactive Black 5, Reactive Blue 160 by *Lentinus squarrosulus* AF5 and Assessment of Toxicity of the Degraded Metabolites

Anshu Mathur, Chandrachur Ghosh, Partha Roy, Ramasare Prasad, Rajesh Pratap Singh*

Department of Biosciences and Bioengineering, Indian Institute of Technology Roorkee, Roorkee, India
Email: *r.singh@bt.iitr.ac.in

How to cite this paper: Mathur, A., Ghosh, C., Roy, P., Prasad, R. and Singh, R.P. (2024) Bioremediation of Textile Azo Dyes Amido Black 10B, Reactive Black 5, Reactive Blue 160 by *Lentinus squarrosulus* AF5 and Assessment of Toxicity of the Degraded Metabolites. *Advances in Microbiology*, **14**, 137-161.
https://doi.org/10.4236/aim.2024.142011

Received: January 4, 2024
Accepted: February 26, 2024
Published: February 29, 2024

Abstract

Bioremediation is an eco-compatible and economical approach to counter textile dye menace. The isolated *Lentinus squarrosulus* AF5 was assessed for decolourization of textile azo dyes, and had shown ~93%, 88% and 70% decolorization of Reactive blue 160 (RB160), Reactive black 5 (RB5) and Amido black 10B (AB10B) respectively. Further analysis using UV-vis, HPLC, and FTIR, ^{1}H NMR had shown the degradation of the dyes. Toxicity analysis of the metabolites was performed using seed germination and plant growth on two agriculturally important plants Guar (*Cyamopsis tetragonoloba*) and wheat (*Triticum aestivum*) as well as cytotoxicity analysis using the human keratinocyte cell line (HaCaT). The dye mix appeared inhibitory for seed germination (20% - 40%), whereas metabolites were non-inhibitory for germination. Treatment of HaCaT cells with of dye mix and metabolites led into 45% and ~100% of cell viability of HaCaT cells respectively. Therefore, metabolites following degradation of the dye mix were observed to be non-toxic.

Keywords

Lentinus squarrosulus AF5, Azo Dyes, FTIR, ^{1}H NMR, Catabolism, Cytotoxicity

1. Introduction

Rapid industrialization leading into environmental pollution, particularly from the, leather, textile, food, and agricultural sectors, is a major concern. Specifically, over 90% of the effluents containing dyes are generated from the textile sector

and contain distinct contaminants, including surfactants, acids or bases, heavy metals, salts, suspended solids, and dyes [1] [2] [3] [4]. Toxicity due to the dyes are not only aesthetically unacceptable, but also hazardous to flora and fauna [5] [6] [7].

Reactive dyes are typically used by the textile industry owing to their fastness and better washability and extensive colour spectrum [8] [9]. The group of dyes commonly used in textile finishing are azo dyes due to their excellent fixing quality, resistance to microbial destruction and high photolytic stability. These dyes pose environmental and health hazards due to their impact as carcinogenic, toxic and mutagenic agent [10] [11]. The release of colored textile effluents into lakes and rivers reduces the amount of dissolved oxygen in the water and creates adverse conditions in aquatic ecosystems [12] [13].

According to [14], nearly 10% - 25% of the dye is still unbound and is discharged as effluent. Moreover, sectors such as leather cosmetics, pharmaceuticals, and food, also employ azo dyes, thereby generating wastewater [15]. The textile sector leads to air and water pollution through the emission of nitrous oxide, sulfur dioxide and carbon monoxide. When discharged dyes enter water bodies, it imparts colour, affects photosynthesis and leads into harmful effects on ecosystem [16].

The present study was undertaken to evaluate the isolated strain *Lentinus squarrosulus* AF5 for its ability for catabolism of azo dyes as well as to assess the toxicity of the metabolites following degradation.

2. Materials and Methods

Dyestuff and Chemicals

The dyes used in the study consist of Amido Black 10B (AB10B), Reactive Black 5 (RB5), Reactive Blue 160 and were procured from MP Biomedicals (USA), Tween-80, Veratryl alcohol, and other chemicals were procured from HiMedia (Mumbai), India. All the chemicals and reagents used were of the highest analytical grade available.

Strain:

The strains *Lentinus squarrosulus* AF5 was isolated from the site in and around Roorkee (29.8543˚N, 77.8880˚E) Uttarakhand, India, that was discharged with effluents from the dyeing process. Strain AF5 was maintained on potato dextrose agar (PDA) medium [17].

Analytical procedures:

To find out if the dyes following incubation undergo catabolism, *L. squarrosulus* AF5 was grown in Kirk's medium and the dye or dye mix (500 $mg{\cdot}L^{-1}$) was added after 48 h of growth and subjected for 72 h of further incubation at 30˚C under shaking (200 rpm). Supernatants were further analyzed for dye degradation.

High Performance Liquid Chromatography:

The supernatant was collected and extracted with equal volume of diethyl

ether and dried over anhydrous Na_2SO_4, evaporated to dryness in rotary evaporator. The resulting crystals were dissolved in a small volume of HPLC grade methanol and analysis was performed in an isocratic Waters 2690 (UK) on a C18 hydrosphere column (Symmetry, 4.6 × 250 mm). HPLC grade methanol was used as the mobile phase with a flow rate of 0.50 ml·min^{-1} for 10 min. Filtered sample (10 µl) was manually injected into the injector port, UV-Visible detector was used for the analysis [18].

Fourier Transform Infrared Spectroscopy Analysis:

The extracted metabolites were analyzed using FTIR (Perkin-Elmer 1600, USA). Extracted metabolites were mixed with HPLC grade potassium bromide (KBr) in a ratio of 5:95, and ground in an agate pestle and mortar and processed through a hydraulic press. FTIR analysis was performed using a mid-IR region (400 - 4000 cm^{-1}) [17] [19] [20].

Nuclear Magnetic Resonance Analysis:

The extracted metabolites were dissolved in appropriate volume of D_2O for ^1H NMR analysis using by Bruker Avance AMX-500MHz FT-NMR spectrometer, USA). The data obtained were processed using TOPSPIN version 3.0 software (Bruker) [19] [21].

Phytotoxicity assessment:

Seed germination using two agriculturally significant plants Guar (*Cyamopsis tetragonoloba*) and wheat (*Triticum aestivum*) were performed to examine the degree of toxicity of azo dyes and its degraded intermediates. The experiments were conducted in petri dishes using Whatman grade 1 filter papers that had been dipped in 5 mL of the dye solutions and extracted metabolites (500 mg·L^{-1}). Ten healthy seeds in each plate were placed initially for 72 h in dark to promote germination, 5 ml of dye or metabolites solutions (500 mg·L^{-1}) were used to wet germination setup per day.

Control sets were exposed with distilled water. All the group of samples were subjected for incubation in triplicates in similar environmental setups. After seven days, the germination rate and the size of the shoot and root were measured [22] [23] [24] [25] [26].

$$\text{Germination}(\%) = \text{No. of seeds germinated}/\text{No. of seeds sowed} \times 100 \quad (1)$$

Cell toxicity assay:

The DMEM media and the antibiotic solutions used in this study were procured from Himedia, India. Fetal Bovine Serum and trypsin-EDTA solution used in the cell culture were procured form Gibco, Sigma. All the other chemicals and reagents including MTT, used in this study were obtained from Himedia, India.

Cell culture:

Human keratinocytes (HaCaT) cells were grown in DMEM high glucose medium with 10% FBS and 1.1% antibiotic-antimycotic in a humid incubator with 5% CO_2 at 37˚C. Cells were grown up to 80% - 90%, collected using trypsin-EDTA (0.25%), and then plated for assays. Medium was replenished on

every alternate day.

Treatment:

5×10^3 cells were seeded in each well of a 96 well plate and incubated for 24 hours. The dye mix or metabolites extracted after degradation, collected at different times (24, 48, 72 and 96 hours) were dosed in desired concentrations (70, 110, 150, and 200 µg/ml) for another 24 hours in DMEM media. Wells having only DMEM media with no cells were used as blank. The cells were incubated with dye mix or extracted metabolites for 24 hours in DMEM media at 37˚C.

MTT assay for cell viability:

MTT (3-(4,5-Dimethylthiazol-2-yl)-2,S-diphenyltetrazolium bromide) assay was carried out to assess the cell cytotoxicity [27]. After the 24 hours of incubation with dye mix or extracted metabolites, 20 µL of MTT (5 mg/ml) was added and incubated for 4 h. DMSO (200 µl) was added to each well to dissolve the formazan crystals that had formed inside the cells. The absorbance of purple colored formazan crystal was measured at 570 nm using the microplate reader, cell cytotoxicity was measured as the percentage of cell viability compared to the control group.

$$\begin{aligned}&\text{Percentant of cell viability}\\&= \text{Mean of O. D of trated cell}/\text{Mean OD of control} \times 100\end{aligned} \tag{2}$$

Cell morphology:

A 6-well culture plate was seeded with exponentially growing HaCaT cells (1×10^3 cells/well). The cells were treated with dye mix or extracted metabolites (70 - 200 $\mu g \cdot mL^{-1}$) for 24 h in DMEM media at 37˚C [28]. The media was then withdrawn from the wells, cells were washed with phosphate buffered saline, and the morphology of the cells was examined.

3. Results and Discussion

Dye degradation analysis: UV-Visible spectroscopy:

UV-vis spectral analyses of the AB10B, RB5, RB160 (100 $mg \cdot L^{-1}$) at varying time intervals had shown that the dyes get decolorized following 0 - 72 h of incubation. The absorbance at 400 - 700 nm refers to the n/p* transition of the azo and hydrazone forms, which is the source of the colour of azo dyes and is used to measure the decolorization. These transitions in the naphthalene and benzene rings of azo dyes were considered to be responsible for the absorbance between 200 and 400 nm. The degradation of the dye's aromaticity is shown by the decline in its absorption. **Figure 1(a)** shows that at both *i.e.* at 200 - 400 nm and 400 - 800 nm, the levels of dye decreases steadily with increasing time intervals due to the progressive decoloration and catabolism of the dye. Similar observations have indicated the gradual decrease of the absorbance peak of AB10B at 618 nm and decolourization of AB10B upon degradation, within a few hours in parallel to the formation of pink color [29] [30] [31].

UV-Vis analysis for RB5 denoted that aryl and naphthalene-like moieties, as well as chromophoric azo linkages, could be the indicative of the characteristic

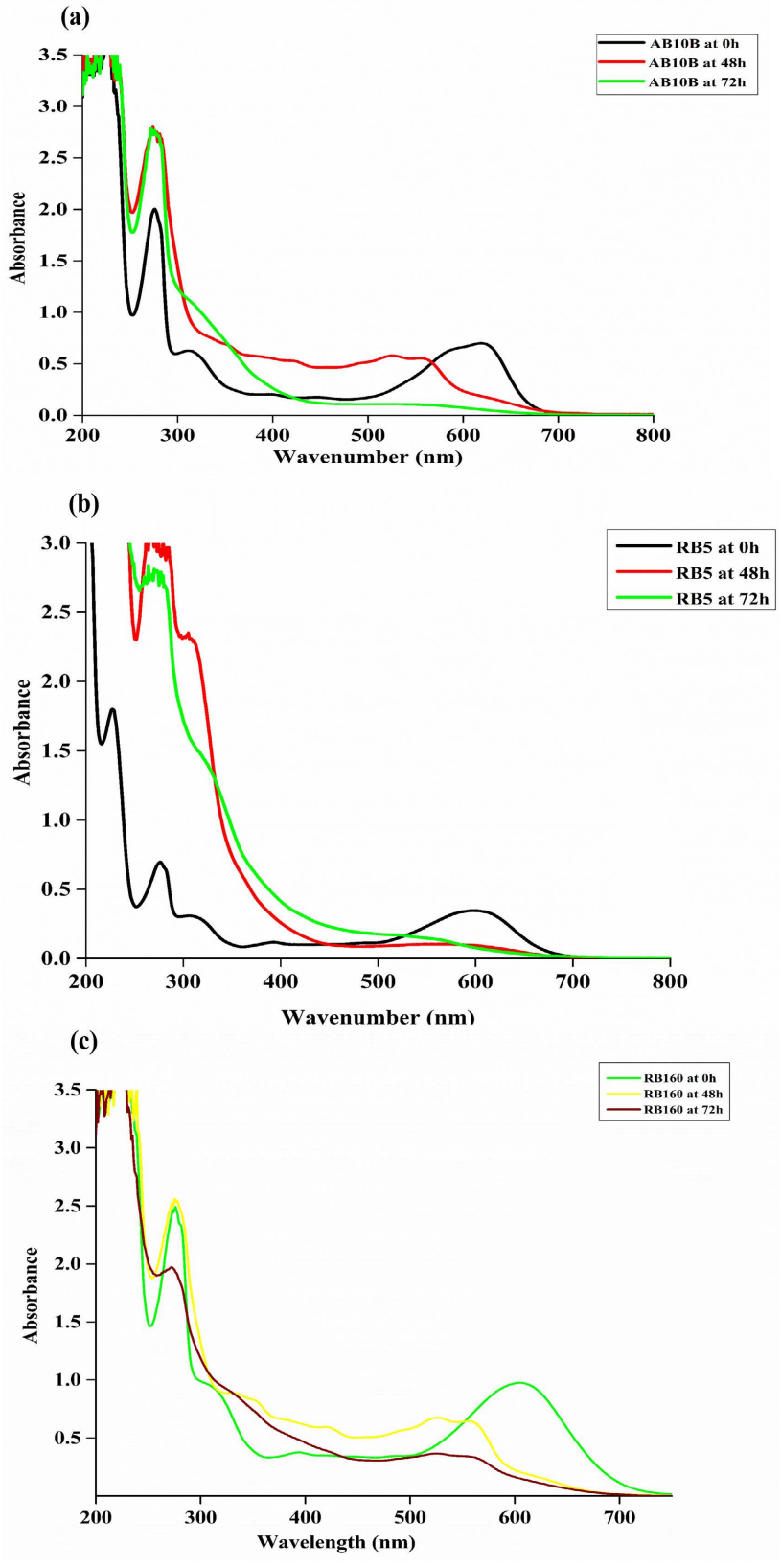

Figure 1. UV-Visible Spectral analysis (200 - 800 nm) of the culture supernatant at varying time intervals from medium containing the Amido Black 10B (a), Reactive Black 5 (b), Reactive Blue 160 (c) by *Lentinus squarrosulus* AF5.

peaks at 597 and 310 nm [32]. RB5 appears to be catabolized following 72 h of incubation, possibly accompanied with metabolic intermediates. These catabolites had earlier been ascribed to be aromatic amines with the adsorption maxima at 254 nm and the putative product elucidation for the azo dye reduction (**Figure 1(b)**) [33].

The spectra of RB160 demarcate peak at 278 nm and the other at 618 nm. The major peak observed at 618 nm had decreased gradually and finally disappeared indicating the decolourization of the dye. However, peak at 278 nm had gradually decreased possibly denoting the putative catabolic products (**Figure 1(c)**) [34].

HPLC Analysis of AB10B, RB5, RB160 metabolism:

The strain *L. squarrosulus* AF5, during incubation was added with AB10B, RB5, RB160, the supernatants were collected at different time intervals and centrifuged (10,000 rpm, 10 min), and then extracted with equal volumes of dicholoether, evaporated to dryness using Na_2SO_4. Dried crystals were further dissolved in HPLC grade methanol and used for chromatographic analyses [35].

Catabolism of Amido Black 10B:

The AB10B are extensively employed in textile sector for coloring the synthetic fiber like, polyesters, nylon as well as natural fiber such as wool, cotton, silk, and textile printing. Other industry usage comprises of dyeing of soaps, casein, anodized aluminum, writing ink and wood stain. Its structure includes azo, anilino, phenolic, and sulphonate groups. It is an acidic diazo dye with strong photo- and thermal stability. This dye is well known to cause irritation to the skin, eyes, and respiratory system in humans [29] [30].

HPLC analysis of the AB10B dye had shown peaks with retention times of 6.2 and 6.4 min (**Figure 2(a)**), while the supernatant collected following incubation of dye for 24 h and 72 h with strain AF5 had denoted peakes mainly with retention times of 5.21, 7.91 and 6.81, and 3.89 respectively (**Figure 2(b)** & **Figure 2(c)**). During the degradation process, the native peak for AB10B had decreased, and some new peaks appeared, thus indicating the generation of degradation intermediates.

As the reaction continued, the intermediate products formed in the initial reaction stage possibly undergo further degradation, leading to the formation of other components. This denotes the dyes presumably undergoing catabolism and similar observation denoting putative catabolites had earlier been reported consisting of phenoloics and aromatic derivatives [29].

Catabolism of Reactive Black 5:

Reactive dyes are widely used for processing cotton, other cellulosic fibers in the dyeing industry. It exhibits high water solubility, and its enormous discharge in water bodies may have an adverse impact on water and human bodies. These dyes are capable of forming covalent linkages with -NH, -SH, OH in the textile fiber made up of cotton, silk, nylon and wool [36].

HPLC analysis of the RB5 had demarcated the major peaks with retention times of 4.14, 7.08 (**Figure 3(a)**) while incubation had led into disappearance of

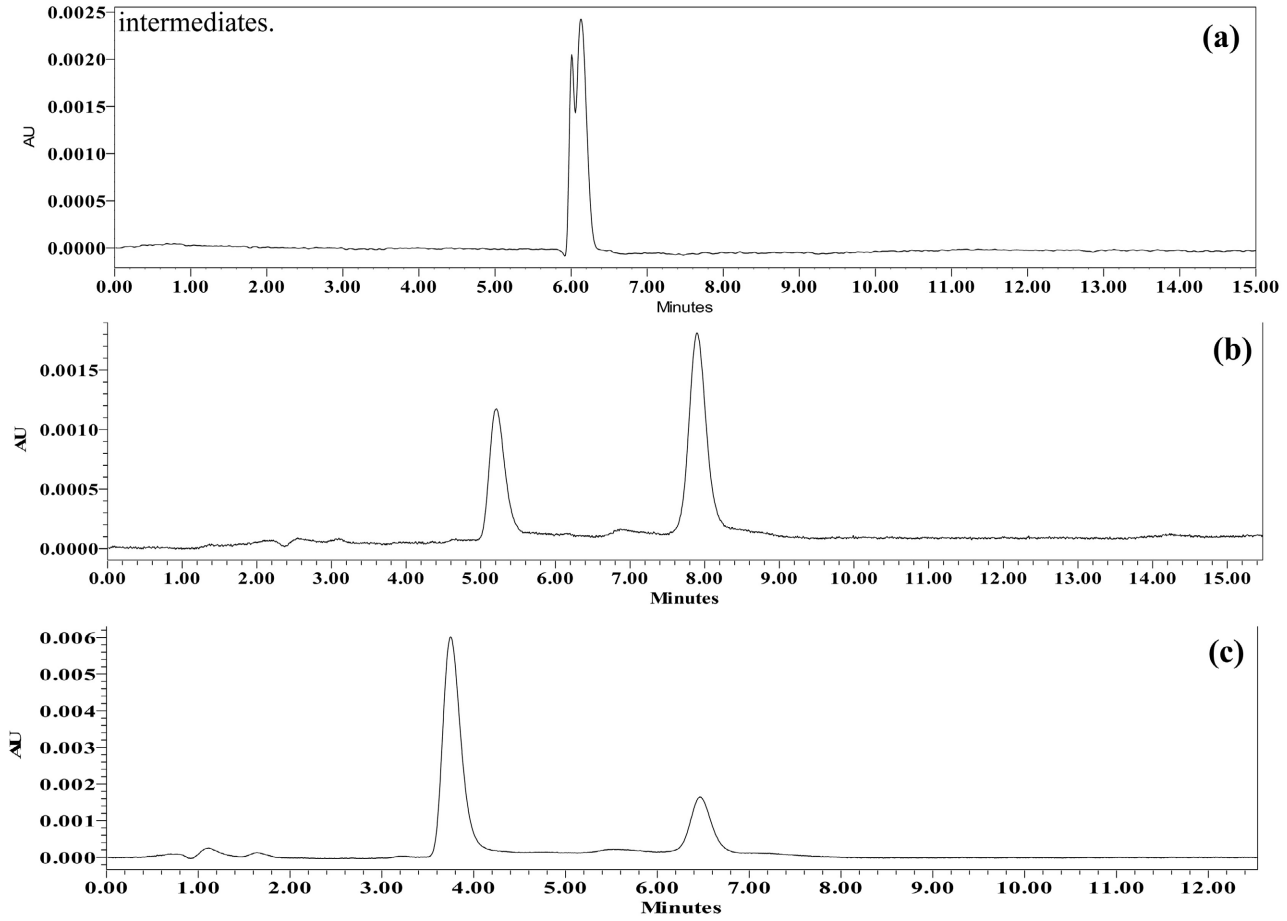

Figure 2. HPLC profile of AB10B (a), extracted metabolites at 24 h (b) and 72 h (c) by *L. squarrosulus* AF5.

major peak and the six peaks with retention times of 2.88, 4.07, 5.18, 6.32, 8.08, 9.24 after 24 h had appeared along with minor peaks (**Figure 3(b)**). Prolonged incubation had shown the distinct peaks 2.77, 5.48 after 72 h (**Figure 3(c)**) and disappearance of the two earlier peaks that demarcate the further mineralization of the parent dye RB5.

Catabolism of Reactive Blue 160:

RB160 is a diazo commercial dye, generally employed for coloring viscose, cotton, flex, and jute but not suitable for wool, silk, and polyesters. There are very few studies on the decolorization and catabolism of RB160.

Among the azo dyes, those with the triazine group are particularly essential due to the well-known resistance of the s-triazine to light-induced fading [34] [35] [36] [37].

The HPLC profile of RB160 dye (**Figure 4(a)**) shows notable peak with the retention time of 6.41. Following incubation with *L. squarrosulus* AF5 a considerable decline in the major peak represented the mineralization of the dye. As a result of catabolism, after 24 h, intermedites formed displayed the main peak at a retention time of 5.16 min and minor peaks with retention times of 2.53, 6.12, 7.86, 8.82, and 9.93 min (**Figure 4(b)**). The primary peak dissipates after 72 h

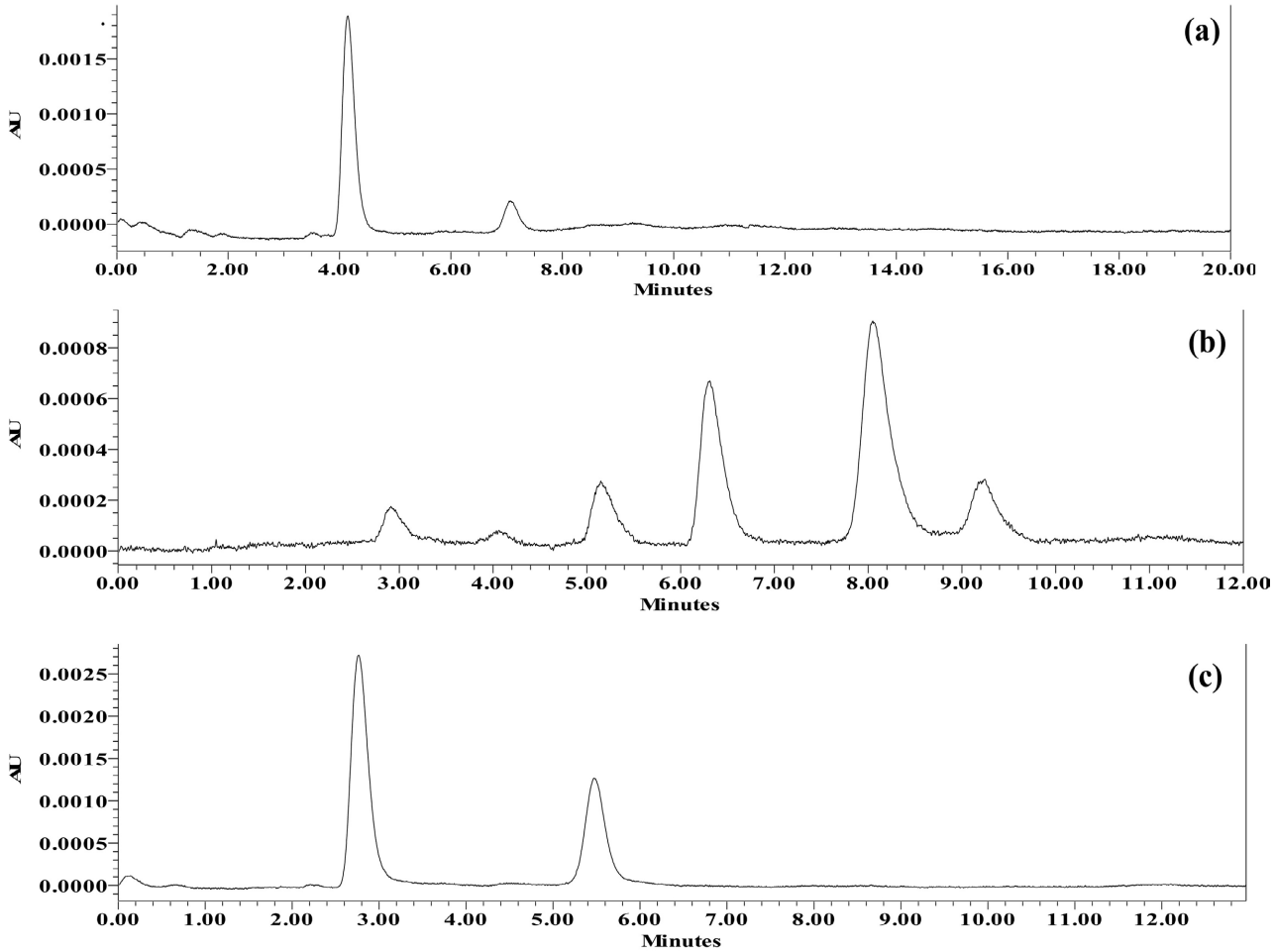

Figure 3. HPLC profile of RB5 (a), extracted metabolites at 24 h (b) and 72 h (c) by *L. squarrosulus* AF5.

and the resultant peaks appear with retention times of 11.27, 11.96, 12.03 (**Figure 4(c)**) indicating the catabolism of the dye.

4. FTIR Analysis

Amido Black 10B:

FTIR spectral analysis of the dyes used along with extractants following incubation of dyes with strain AF5 was performed. AB10B show the distinctive broad peak at 3396 cm^{-1}. Peak was recorded because of the -OH groups presents which shifted at 3443 cm^{-1} and peaks around 657 cm^{-1} denote the aromaticity of the compounds (**Figure 5(a)**). As a result of the presence of (symmetric and asymmetric) stretching of the -CH_2 group, bands at 2947 cm^{-1} and 2834 cm^{-1} were observed, these bands shifted at 2349 cm^{-1} and 2095 cm^{-1} as a result of degradation of Amido Black 10B [38]. The strong peak was attributed at 1081 cm^{-1} to the stretching of C-N groups and vibrations of the aliphatic amine as reported earlier [39]. 1639 cm^{-1} (N-H deformation), 1403 cm^{-1} (C-H deformation in asymmetric CH_3), peaks at 699 - 643 cm^{-1} as indicated earlier denote the loss of aromaticity (**Figure 5(b)**). Therefore, these observations had indicated

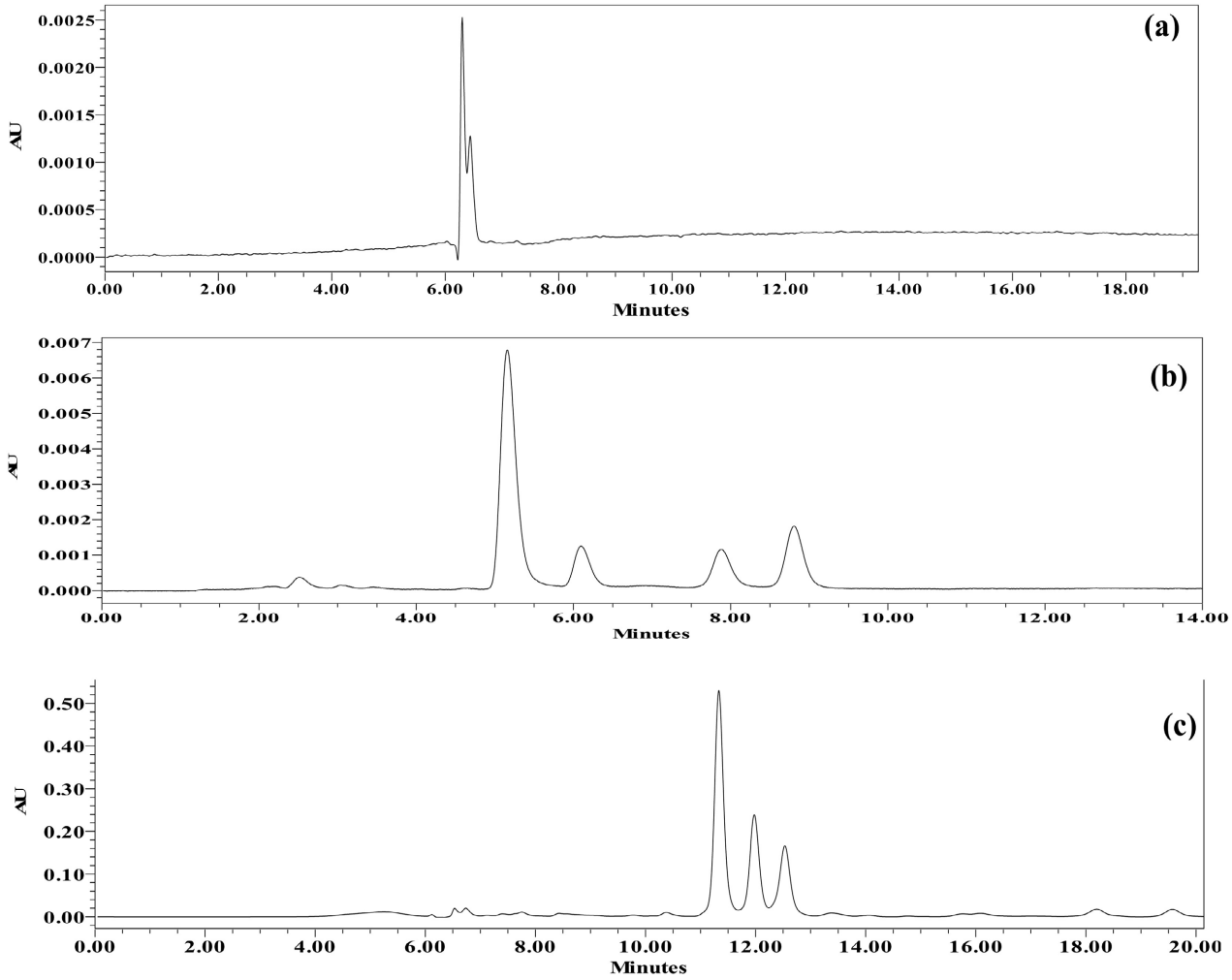

Figure 4. HPLC profile of RB160 (a), extracted metabolites at 24 h (b) and 72 h (c) by *L. squarrosulus* AF5.

that azo dyes following incubation with strain AF5 appear to undergo degradation. The peak at 1028 cm^{-1} was attributed due to presence C-N group stretching and the vibration of aliphatic amine was shifted to 1081 and 1033 cm^{-1} after the adsorption of dyes [13].

Similar observations had earlier been obtained in which the C=C, characterstics peak at 1641 and 657 cm^{-1} peaks were shifted to 1639 and 1403, 699 cm^{-1} and azo bond characteristic peak at 1450 - 1411 cm^{-1} in the dye molecules and was further disappear after degradation [40]. These findings suggest that the strain *L. squarrosulus* AF5 appear to be a potential strain for catabolism of azo dyes.

Reactive Black 5:

FTIR spectrum of the dye exhibits the typical peak of -OH as well as -NH vibrational stretching at 3435 cm^{-1}. The distinctive peaks at 2917 cm^{-1} and 2855 cm^{-1} are associated with the $-CH_3$ asymmetric and $-CH_2$ symmetric vibrational stretching respectively. At 1629 cm^{-1}, there is a distinctive peak for the C-C for aromatic ring. The peak is associated with the azo linkage stretching at 1458

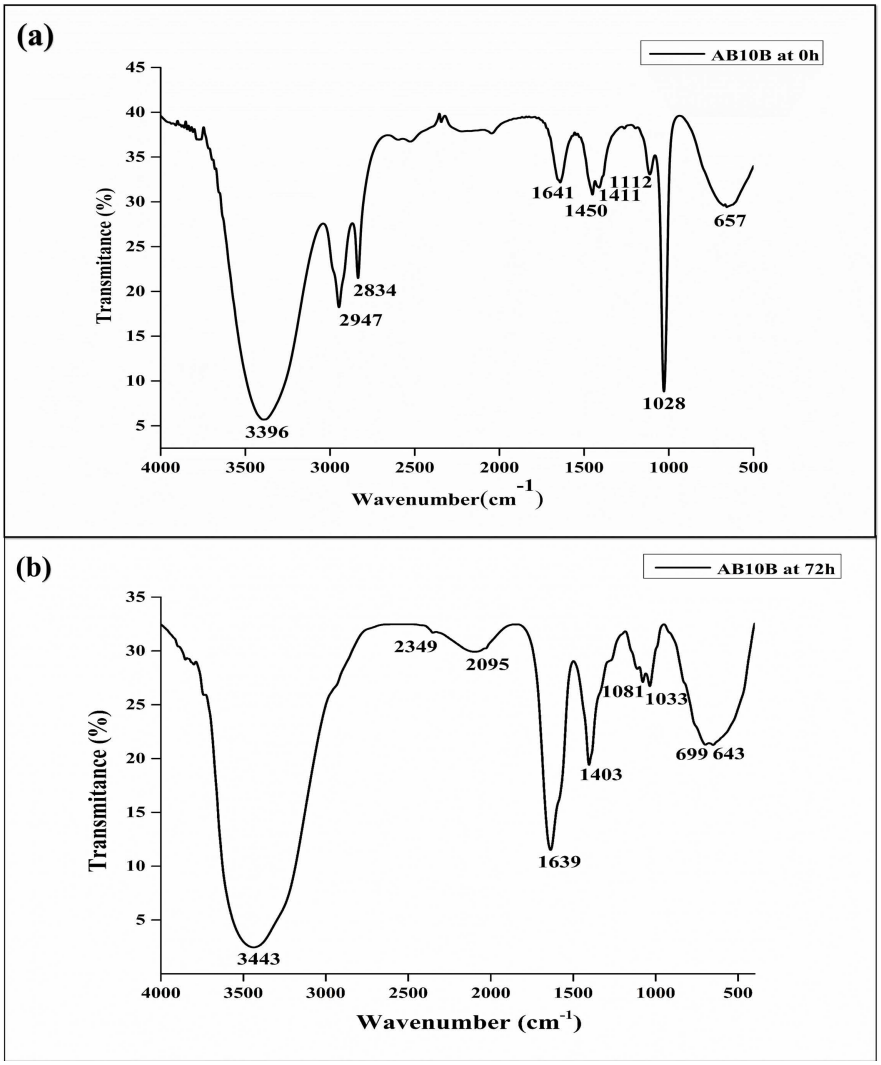

Figure 5. FTIR spectroscopy of Amido Black 10B (a) and metabolites (b).

cm^{-1}. The characteristic FTIR signal, which occurred at 1052 cm^{-1}, demonstrated that RB5 dye is containing the sulfoxide group (**Figure 6(a)**) [20] [36] [41].

In contrast, the FTIR demonstrates the functional groups of the reaction intermediates that were produced as a result of the dye degradation and are indicated in the corresponding spectrum peaks (**Figure 6(b)**). The spectral behavior seen reflects as reported in earlier denoting dye degradation [36] [41]. There is a peak at 3385 cm^{-1} for N-H stretching, 1259 cm^{-1} for CO stretching, and 1642 cm^{-1} for N-H bending. The reductive breakage of the -N=N- bond following degradation is shown by the FTIR possibly generating a primary amine as the intermediates. This is consistent with disappearing of the peak at 1458 cm^{-1}, indicating that the azo link is disrupted. The RB5 dye and possibly the $-CH_2$ groups in the short hydrocarbon chains of the byproducts display symmetric and antisymmetric C-H stretching vibrations at a wavelength of around 2927 cm^{-1} [20].

The disappearance of Reactive black 5 characteristic bands may be assigned to

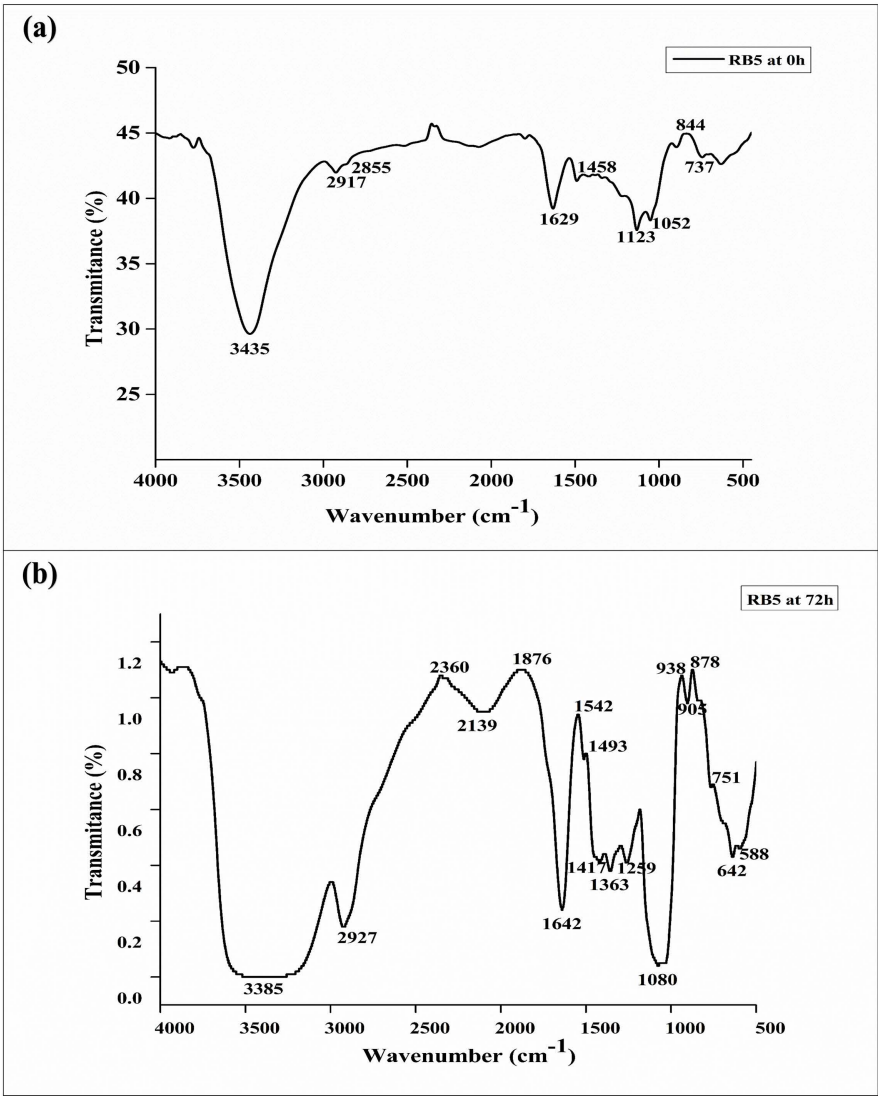

Figure 6. FTIR spectroscopy of Reactive Black 5 (a) and metabolites (b).

the catabolism through the breaking of C=O bond and O-H bonds representing peaks at 1642 cm^{-1}, and 1363 cm^{-1}, respectively. These peaks indicate the quinone and phenolic derivatives following RB5 biodegradation as observed earlier [42]. Thus, azo (N=N) linkage (responsible for the color), aromatic amines, -NH_2, and -RSO_3 get mineralised after 72 h of cultivation, it is evident due to decrease in colour intensity and also the variation of colour from dark blue to violet. Similarly, the variation in colour intensity along with the azo linkage has been observed earlier during the degradation of RB5 by *Trichosporon akiyoshidainum* [43].

Reactive Blue 160:

The FTIR spectrum analysis of the Reactive Blue 160 indicates particular peaks for secondary amides (N-H stretching), nitroso compounds (N=N stretching), sulfoxide (S-O stretching), and C-Br stretching vibrations at 3426 cm^{-1}, 1449 cm^{-1}, 1023 cm^{-1}, and 617 - 620 cm^{-1}, respectively (**Figure 7(a)**). Several

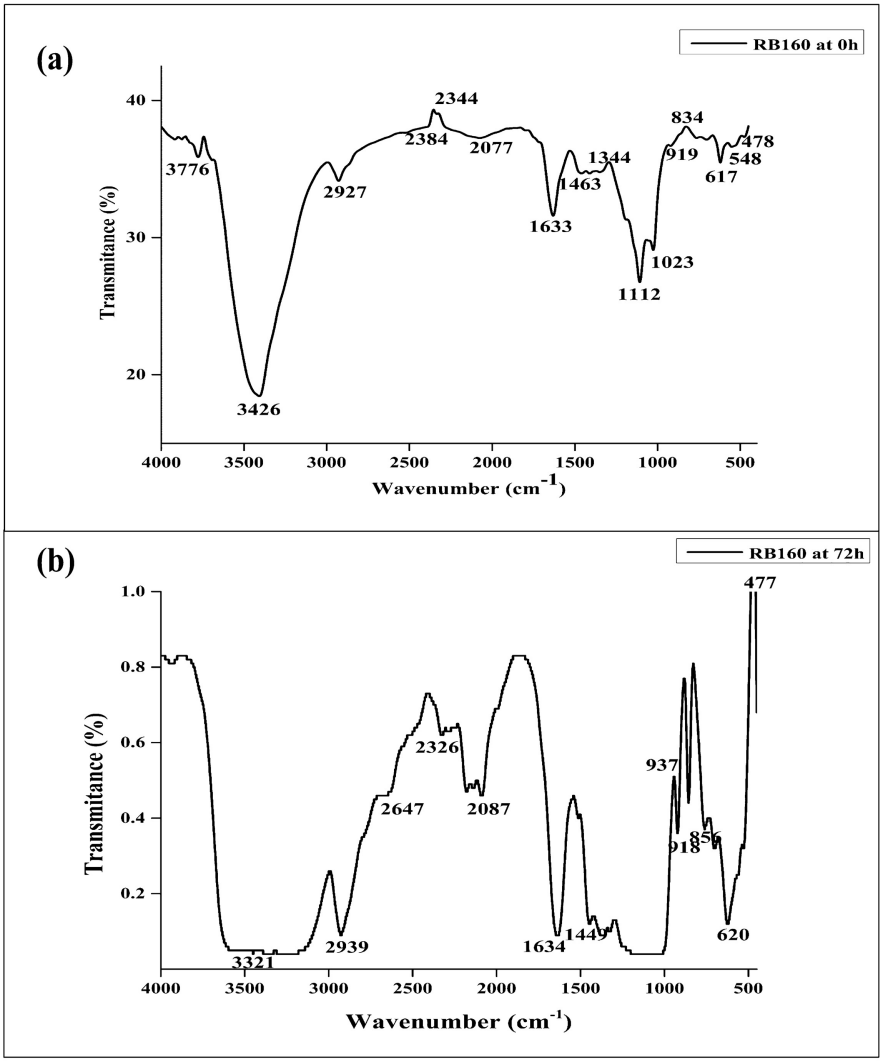

Figure 7. FTIR spectroscopy of (a) Reactive Blue 160 (b) metabolites.

peaks between 900 and 620 cm^{-1} confirmed the RB160's aromatic nature. Prominent peaks were noticeable in the FTIR spectrum of decolorized Reactive Blue 160 at 3321 cm^{-1} for secondary amides (N-H stretching), 2939 cm^{-1} for alkanes, 2647 cm^{-1} for aldehydes, 1634 cm^{-1} for N-H deformation (**Figure 7(b)**).

In addition, the peaks at 1344 cm^{-1} and 1112 cm^{-1} dissipated indicating the separation of S=O bonds from SO_3 groups. These findings indicated that azo linkages of RB160 were reductively cleaved by oxidative reductases. The azo bond cleavage is indicated by the disappearance of peak at 1463 cm^{-1} [19] [44].

^{1}H NMR spectra analysis:

A Bruker 400 MHz spectrometer was used to evaluate the ^{1}H NMR data of azo dyes and their degradation products using D_2O as the solvent. ^{1}H NMR spectroscopy provides useful information regarding major functional groups present in azo dyes and in the degraded products.

^{1}H NMR spectra analysis for Amido black 10B:

The low field of azo dye AB10B displays a singlet at 9.85 ppm, that can be due

to the proton of the hydroxyl group. The presence of doublet signals at 7.56 to 7.58 ppm and triplet signals at 7.40 - 7.43 ppm are from the naphthylic hydrogen and signals at 5.6 shows the amine proton of the dye molecule (**Figure 8(a)**). ^{1}H-NMR spectrum of the dye intermediates show that appearance of protons as

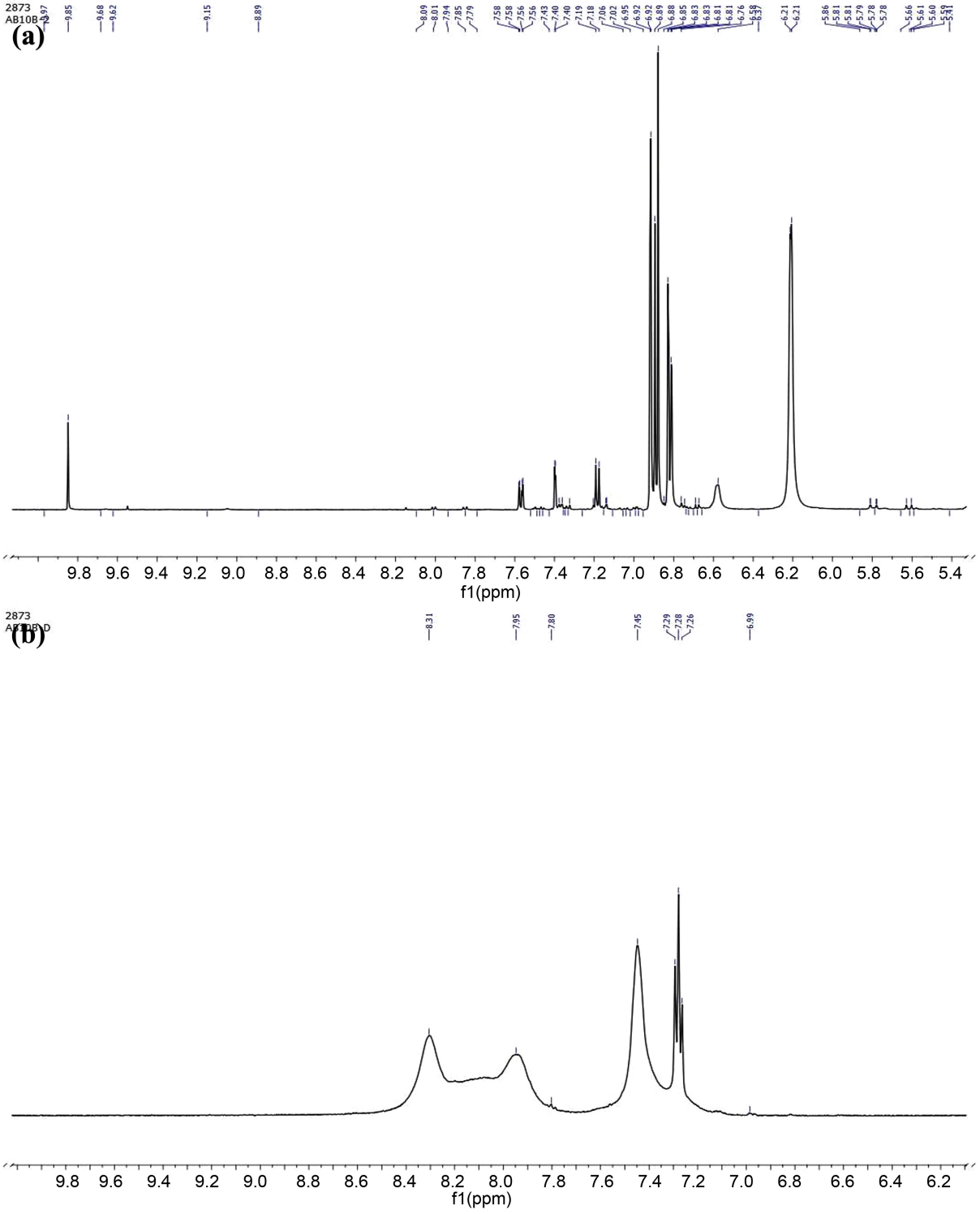

Figure 8. ^{1}H NMR spectrum of AB10B dye (a) and the intermediates (b).

triplet signals in the region at 7.26 - 7.29 depicted the naphthalene protons and signals at 7.95 and 8.31 ppm from the benzene protons that denote the possible intermediates indicates due to the chemical shifts observed in the formation of dye intermediates. It's observed that the chemical shift for protons of 1-naphthalene after degradation declined possibly due to shielding of aromatic rings of the azo dye, and had shifted up field, therefore denoting the formation of dye intermediates. The aromatic protons (benzene and naphthalene rings) depicted in the range of 7.26 - 8.31 ppm and rest of the signals disappeared due to mineralization of the dye (**Figure 8(b)**). The ^{1}H NMR spectra of the extracted samples revealed elimination of signals in the aromatic region (8.31 - 9.97), indicating loss of aromaticity for AR10B after successive dye degradation treatment using the isolated strain AF5 [45] [46] [47].

^{1}H NMR spectra analysis for Reactive Black 5:

^{1}H NMR analysis for RB5 had shown the methylene peaks at 3.97 to 4.06 ppm while aromatic proton peaks at doublet or multiplets (benzene and naphthalene) at 6.18 to 8.27 ppm. The proton of the hydroxyl group is indicated at the 10.40 ppm. The benzene protons of the dye are evident due to the peaks of 6.18 to 8.27 and the ethylene protons in sulfatoethylsulfone group of the dye were considered to be relevant for the prominent peaks of 7 and 8 (**Figure 9(a)**).

The intensity of benzene protons decreased and newer peaks of 6.20 to 6.90 ppm had shown up, for putative metabolites, the ^{1}H NMR spectrum between 2.50 and 3.72 ppm possibly represent aliphatic metabolites (**Figure 9(b)**). Some methine protons in a dimer structure may overlap with methylene peaks like 3.05 to 4.83 because identical methylene protons in a dimer may exhibit distinct chemical shifts depending on the nearby magnetic environment [48]. Furthermore, signals from 5.52 to 7.56 ppm can also be seen in the aromatic areas using the NMR spectra, that for dye intermediates could be attributed to aromatic protons [49].

^{1}H NMR spectra analysis for Reactive Blue 160:

The ^{1}H NMR spectra of untreated dye showed downshift signal at 11.18 from the naphthalene ring hydrogen next to the thionate substituent (**Figure 10(a)**). Furthermore, the intensity of the peaks in the ^{1}H NMR spectra of the metabolites obtained after 72 h of incubation. Treatment gradually decreased, and new signals in the range of 2.64 - 3.74 ppm and 6.20, 6.58 ppm were observed. The loss of signals at the low field zone (6.89 - 9.00) possibly suggests that the dyes undergo mineralization (**Figure 10(b)**). Although, few signals remained in high field zone/lower frequency 2.37 - 4.91 ppm, due to conversion of higher molecular weight constituents into lower molecular weight aliphatic hydrocarbons such as free single bond -CH_3, etc. [1] [46].

^{1}H NMR spectra analysis of Dye Mix:

^{1}HNMR spectroscopic analysis was performed on the dye mix (AB10B, RB5, and RB160) (**Figure 11(a)**). In order to understand the degradation of the dyes, the ^{1}H NMR spectra revealed the 13 distinct hydrogens. The singlet formed at

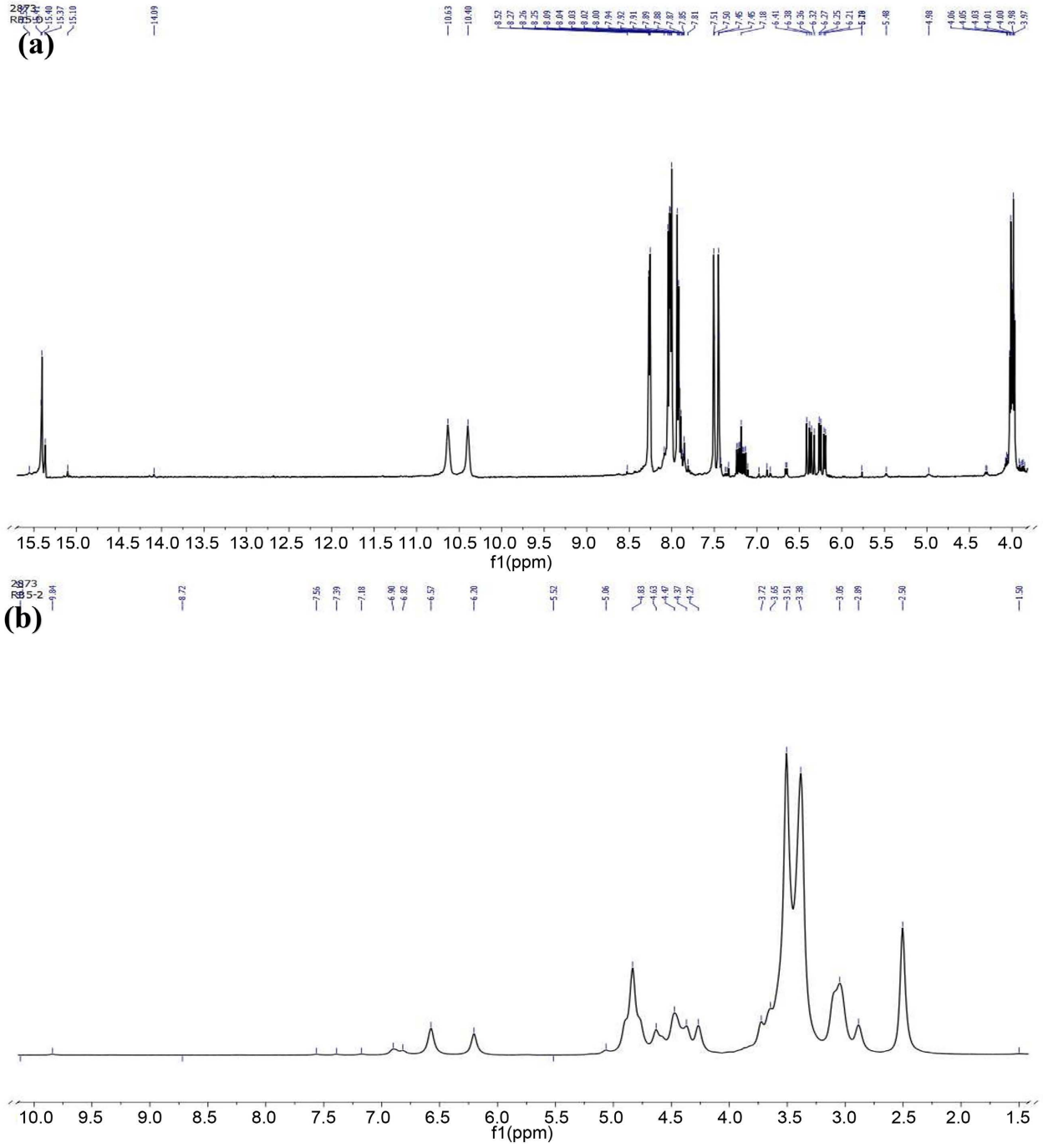

Figure 9. ^{1}H NMR spectrum of RB5 dye (a) and the intermediates (b).

2.89 ppm is from the methine group (=C-) linked to the azo bond. The 2.51 ppm peak is related to CH_2-CN stretching, and the 2.89 ppm and 3.39 ppm peaks are related to the 2H neighbours of CH_2-N. The signal is consistent with (CH_2-O) at 3.72 ppm. Additionally, it had been noted that all proton peaks of aromatic rings de-shielded to the left due to their strong electronegative nature and generated at 6.21 - 7.06 ppm range. The signals at 6.91 ppm and 7.06 ppm represent hydrogen on a benzene ring attached to the N terminal of CN, hydrogen associated

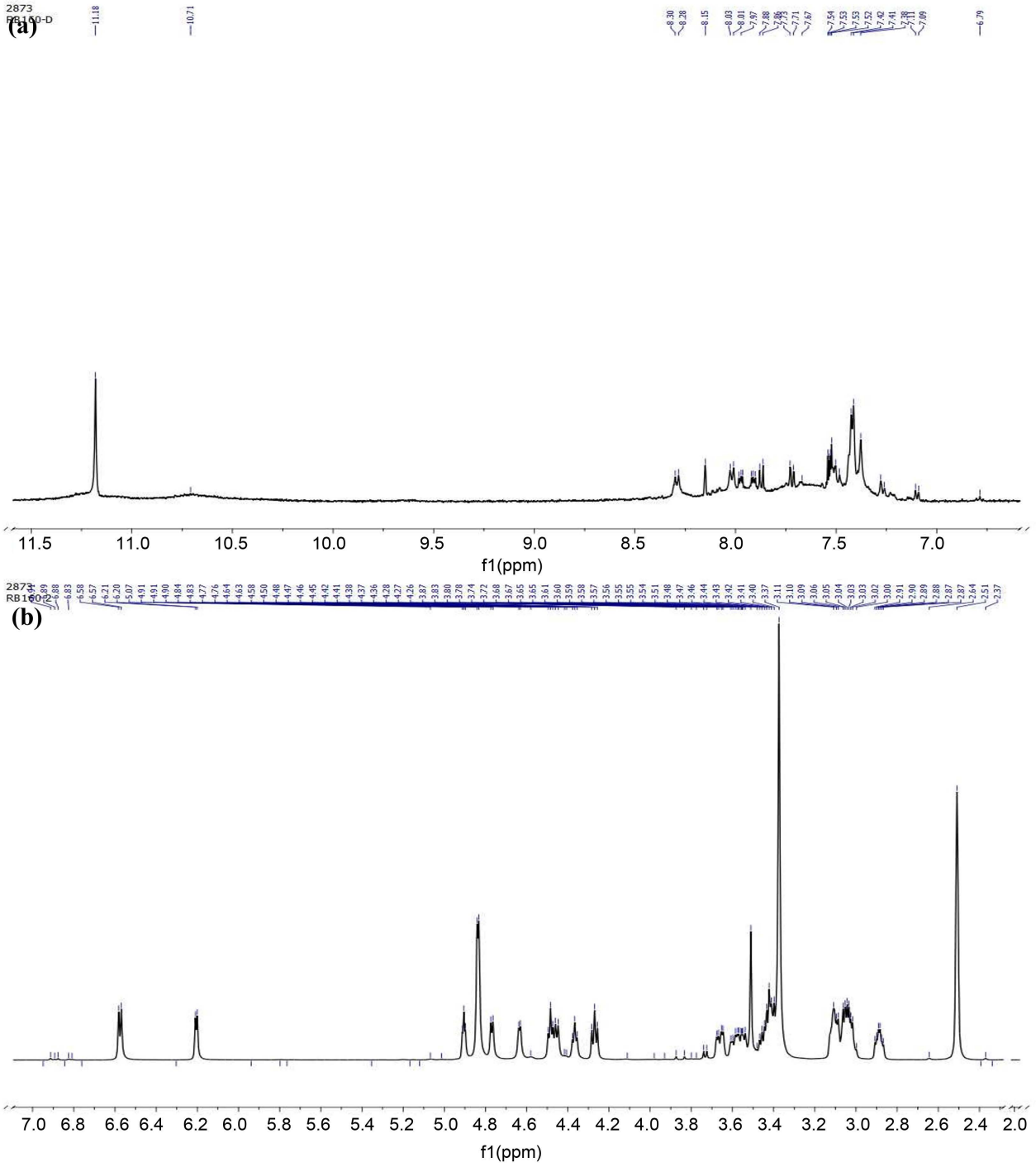

Figure 10. ^{1}H NMR spectrum of RB160 dye (a) and the intermediates (b).

with carbon atoms attached to the N-N and hydrogen atoms on a benzene ring having chlorine, respectively (**Figure 11(b)**). These peaks are made up of three different types of protons, each with a different signal [50]. The disappearance of the signals at the low field zone (6.8 - 9 ppm) indicates the mineralization of the dyes [46]. Furthermore, the signals observed in high field zone/lower frequency range of 1 - 4 ppm denoted the mineralization of the dyes. This has also been

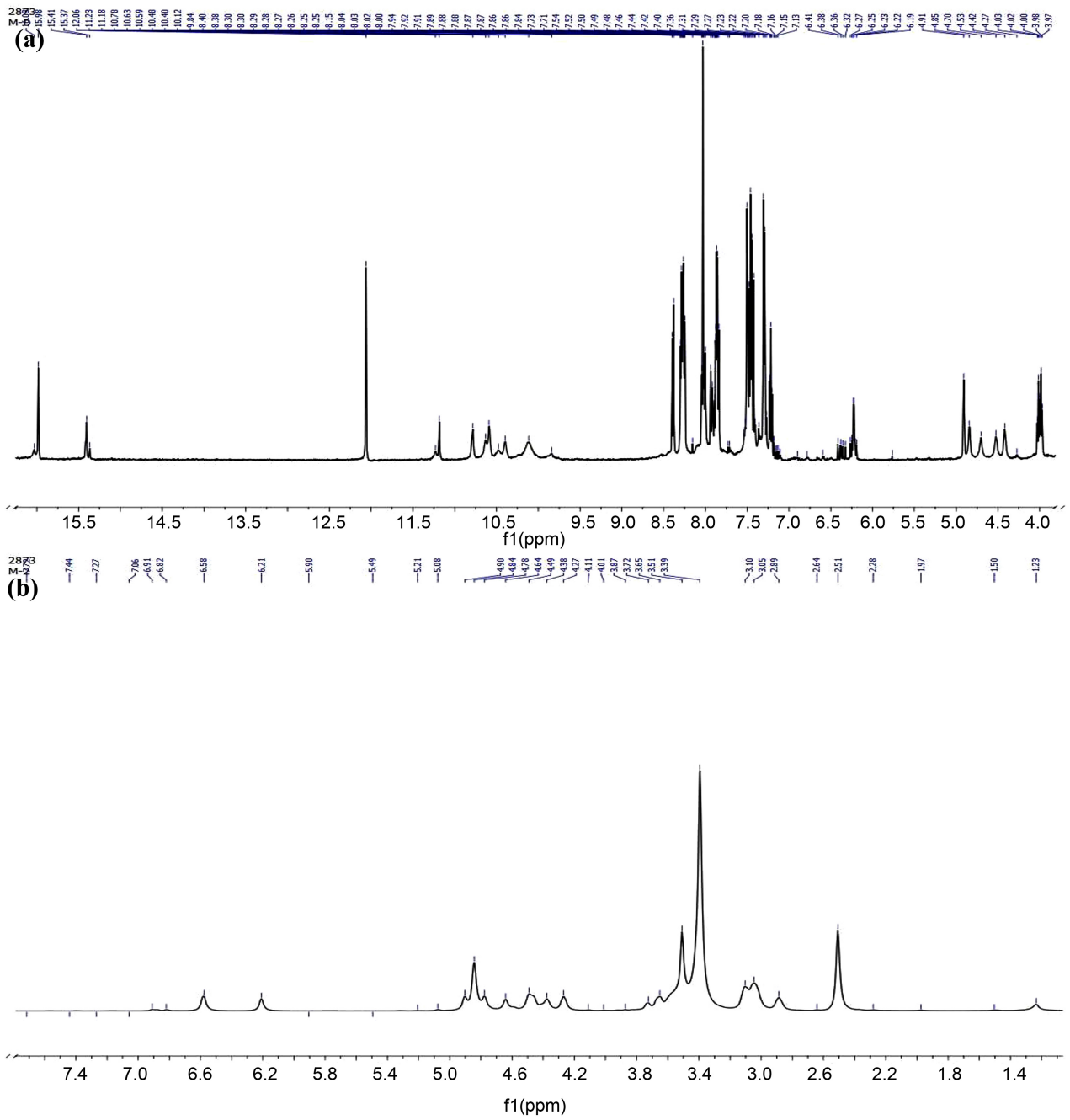

Figure 11. ^{1}H NMR spectrum of Dye mix (a) and the intermediates (b).

earlier observed in the conversion of higher molecular-weight compounds into lower-molecular-weight aliphatic hydrocarbons [1].

Toxicity assessment:

Phytotoxicity assessment:

The germination of seeds and different stages of growth following germination are affected when there are exposed to the toxic substances. In order to evaluate the toxicity of the intermediates following degradation of dyes, two agriculturally important plants Guar (*Cyamopsis tetragonoloba*) and wheat (*Triti-*

cum aestivum) were used for the toxicity studies of the azo dyes and its degraded products. The decreased germination of the both *Triticum aestivum* and *Cyamopsis tetragonoloba* seeds were observed with dye mix as compared to the metabolites. The dye mix had also affected the length of plumule and radical. However, the germination as well as the development of plumule and radical were not affected by the metabolites obtained after 72 h of incubation (**Figure 12(a)** and **Figure 12(b)**).

The phytotoxicity study revealed that there was an inhibition in germination (40%) for the *Triticum aestivum* seed when treated with dye mix (500 $mg \cdot L^{-1}$) as compared to the degradation products (**Table 1**). Dye mix was also inhibitory for shoot (39%) as well as for root (11%) development. *Triticum aestivum*. Similarly dye mix was also inhibitory for the seed germination (20%) for *Cyamopsis tetragonoloba* (**Table 1**). However, metabolites obtained following 72 h of

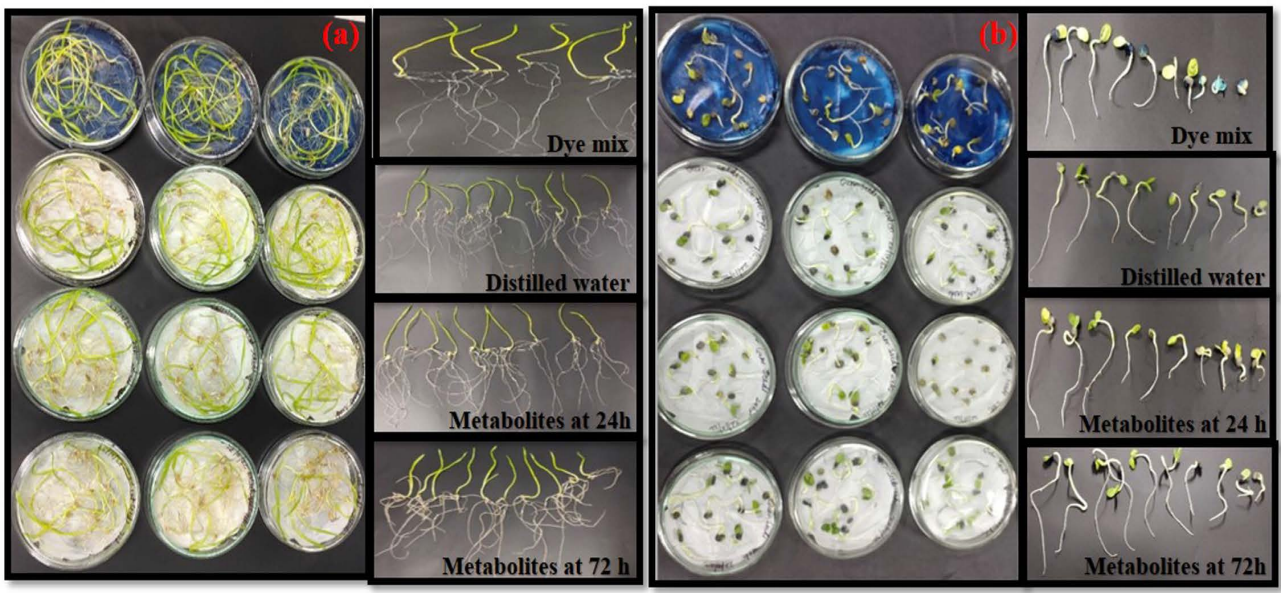

Figure 12. Comparison of phytotoxicity on growth of *Triticum aestivum* (a) and Guar (*Cyamopsis tetragonoloba*) (b) seeds.

Table 1. Phytotoxicity of azo dyes and its degradation products extracted after degradation.

	Triticum aestivum (Wheat)			*Cyamopsis tetragonoloba* (Guar)		
Samples	Germination (%)	Shoot length (cm)	Root length (cm)	Germination (%)	Shoot length (cm)	Root length (cm)
Distilled water	100	2.64 ± 0.11	16.07 ± 0.06	100	1.81 ± 0.60	4.08 ± 0.64
Dye mix (500 mg/L)	60	1.60 ± 0.25	14.26 ± 0.11	80	0.9 ± 0.13	2.61 ± 0.50
Degradation products after 24 h	100	2.60 ± 0.55	14.45 ± 0.56	100	1.09 ± 0.22	3.14 ± 0.86
Degradation products after 72 h	100	2.79 ± 0.49	20.74 ± 0.96	100	2.28 ± 0.14	4.15 ± 1.18

incubation did not affect into seed germination and shoot or root development.

These observations therefore denote that dye mix appear to be toxic for the germination as well as to the growth and development of the plants. Normal germination and development of germinating seeds with the metabolites generated indicate the strain AF5 to be a vital strain for bioremediation applications for synthetic dyes.

Cytotoxicity analysis:

A pivotal model for studying the dermal toxicity is HaCaT cell line, an immortalized epithelial cell line derived from adult human skin that shares many biological traits with healthy human keratinocytes. These cells have been utilized extensively to examine the genotoxicity, mutagenicity, and cytotoxicity of nickel and chromium exposure, as well as skin irritation and skin cancer [28] [51] [52]. We have used this cell line for the toxicity analysis of the azo dyes and also with the metabolites.

Viability assay:

Viability *i.e.* assays using MTT are vital in toxicology for studying cellular response to the toxicants [27]. This assay delineates information on cell death, survival and metabolic activities. A dose response analysis for cytotoxicity assessment of dye mix as well as for the metabolites following 24 h incubation was performed. Increase in antiproliferative effect on cells was observed with increase in the concentration of dye mix. The cell toxicity of the dye mix (70 - 200 $\mu g \cdot mL^{-1}$) for HaCaT cell was observed as the cell viability had decreased (61% - 40%) when the cells are exposed to dye mix (**Figures 13(a)-(d)**).

However, the metabolites generated following degradation of the dyes by the AF5 strain led into marginal decrease in cell viability and thus denoting the non-toxicity of the metabolites (**Figures 13(a)-(d)**). The susceptibility of cells on exposure to dye mix and metabolites was characterized by IC_{50}. The IC_{50} of dye mix was found to be 110 $\mu g \cdot mL^{-1}$ (**Figure 10(b)**) that is comparable to the values observed earlier for the other azo dyes [28].

Cell morphology following dye mix treatment:

The normal cellular architecture was observed for HaCaT cells when the cells were cultured without exposing to dye mix (**Figure 14(a)** and **Figure 14(f)**). The HaCaT cells when added with different concentrations of the dye mix had affected into distinct variations in the cellular morphology. The dye mix-treated cells appeared stretched, elongated, flattened, and skewed, further echinoid protrusions, cellular shrinkage, and granularity were also observed thereby denoting the toxicity of the dye mix (**Figures 14(b)-(e)**). No variations in cellular morphology was observed when the cells were exposed with metabolites obtained following 72 h of incubation (**Figures 14(g)-(j)**).

This further denotes the non-toxicity of the metabolites following mineralization of the dye mix. The degradation of azo dyes by *L. squarusulous* AF5 had led in to catabolism of the dyes as observed earlier and as observed metabolites generated did not impact in to changes in cellular morphology [51].

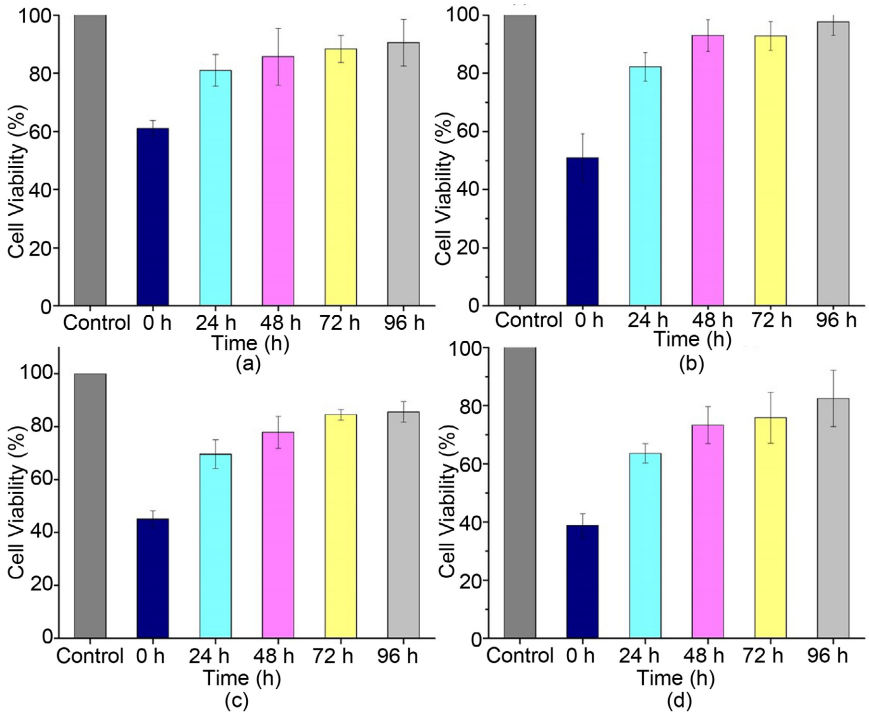

Figure 13. Viability of HaCaT cells by MTT assay on exposure to dye mix and its metabolites ((a) 70 μg·ml^{-1}; (b) 110 μg·ml^{-1}; (c) 150 μg·ml^{-1}; (d) 200 μg·ml^{-1}).

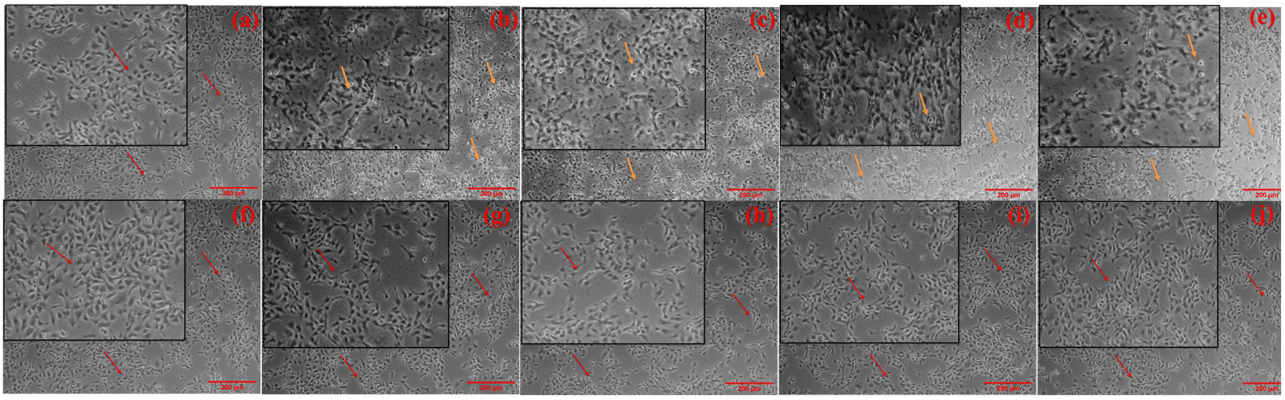

Figure 14. Morphology of HaCaT cells controls ((a), (f)), after exposure to dye mix (70 - 200 μg·ml^{-1}, (b)-(e)) and cytotoxicity of metabolites (at 72 h) on HaCaT cells after exposure (g)-(i) following 24 h of incubation (red arrows indicate normal cellular morphology whereas orange arrows indicate altered morphology; All images are of 20× with scale bar: 200 μm).

5. Conclusion

Bioremediation is a potentially promising substitute for traditional approaches for remediation as it is ecofriendly and relatively economical. *Lentinus squarrosulus* AF5 was observed as potential strain and had a notable ability for degradation of azo dyes. The isolate was earlier observed to degrade the dyes, at the concentration ranging from 100 to 500 mg·L^{-1}. In order to assess the degradation, the extractants were analysed using chromatographic and spectroscopic approaches and thus had denoted that dyes undergo catabolism. Following degradation, the toxicity assessment of the metabolites was evaluated by phytotox-

icity and cell toxicity analyses. These studies had indicated that dyes following degradation undergo mineralization to generate nontoxic metabolites. Thus the strain *Lentinus squarrosulus* AF5 appears to be a notable and potential strain for remediation of the dyes and can enable in developing a process for scaled up degradation of the dyes.

Acknowledgements

The authors AM the Department of Biotechnology (DBT), Govt. of India for the financial assistantship and the Institute Instrument Center (IIC), IIT Roorkee for the instrumentation facility.

Author Contributions

Anshu Mathur: Conceptualization, Investigation, Visualization, Writing—Original Draft.

Chandrachur Ghosh: Cell toxicity assessment and visualization.

Partha Roy: Supervision, Resources.

R. Prasad: Supervision, Resources, Writing—Review & Editing.

R. P. Singh: Supervision, Resources, Visualization, Writing—Review & Editing.

Conflicts of Interest

The authors declare that they have no conflict of interest.

References

[1] Balapure, K., Bhatt, N. and Madamwar, D. (2015) Mineralization of Reactive Azo Dyes Present in Simulated Textile Waste Water Using Down Flow Microaerophilic Fixed Film Bioreactor. *Bioresource Technology*, **175**, 1-7. https://doi.org/10.1016/j.biortech.2014.10.040

[2] Deswal, D., Sharma, A., Gupta, R. and Kuhad, R.C. (2012) Application of Lignocellulolytic Enzymes Produced under Solid State Cultivation Conditions. *Bioresource Technology*, **115**, 249-254. https://doi.org/10.1016/j.biortech.2011.10.023

[3] Sosa-Martínez, J.D., Balagurusamy, N., Montañez, J., Peralta, R.A., De Fátima Peralta Muniz Moreira, R., Bracht, A., *et al*. (2020) Synthetic Dyes Biodegradation by Fungal Ligninolytic Enzymes: Process Optimization, Metabolites Evaluation and Toxicity Assessment. *Journal of Hazardous Materials*, **400**, Article 123254. https://doi.org/10.1016/j.jhazmat.2020.123254

[4] Zaharia, C. and Suteu, D. (2013) Coal Fly Ash as Adsorptive Material for Treatment of a Real Textile Effluent: Operating Parameters and Treatment Efficiency. *Environmental Science and Pollution Research*, **20**, 2226-2235. https://doi.org/10.1007/s11356-012-1065-z

[5] Bharagava, R.N. and Chowdhary, P. (2018) Emerging and Eco-Friendly Approaches for Waste Management. Springer, Singapore, 1-435. https://doi.org/10.1007/978-981-10-8669-4

[6] Gul, R., Sharma, P., Kumar, R., Umar, A., Ibrahim, A.A., Alhamami, M.A.M., *et al*. (2023) A Sustainable Approach to the Degradation of Dyes by Fungal Species Iso-

lated from Industrial Wastewaters: Performance, Parametric Optimization, Kinetics and Degradation Mechanism. *Environmental Research*, **216**, Article 114407. https://doi.org/10.1016/j.envres.2022.114407

[7] Lellis, B., Fávaro-Polonio, C.Z., Pamphile, J.A. and Polonio, J.C. (2019) Effects of Textile Dyes on Health and the Environment and Bioremediation Potential of Living Organisms. *Biotechnology Research and Innovation*, **3**, 275-290. https://doi.org/10.1016/j.biori.2019.09.001

[8] Li, T. and Guthrie, J.T. (2010) Colour Removal from Aqueous Solutions of the Reactive Azo Dye Remazol Black B Using the Immobilised Cells (Shewanella Strain J18 143) Cellulose-g.co-Monomer System. *Journal of Water Resource and Protection*, **2**, 77-84. https://doi.org/10.4236/jwarp.2010.21009

[9] Singh, A.L., Chaudhary, S., Kumar, S., Kumar, A., Singh, A. and Yadav, A. (2022) Biodegradation of Reactive Yellow-145 Azo Dye Using Bacterial Consortium: A Deterministic Analysis Based on Degradable Metabolite, Phytotoxicity and Genotoxicity Study. *Chemosphere*, **300**, Article 134504. https://doi.org/10.1016/j.chemosphere.2022.134504

[10] Chung, K.T. (2016) Azo Dyes and Human Health: A Review. *Journal of Environmental Science and Health, Part C*, **34**, 233-261. https://doi.org/10.1080/10590501.2016.1236602

[11] Forss, J. and Welander, U. (2011) Biodegradation of Azo and Anthraquinone Dyes in Continuous Systems. *International Biodeterioration and Biodegradation*, **65**, 227-237. https://doi.org/10.1016/j.ibiod.2010.11.006

[12] Berradi, M., Hsissou, R., Khudhair, M., Assouag, M., Cherkaoui, O., El Bachiri, A., *et al*. (2019) Textile Finishing Dyes and Their Impact on Aquatic Environs. *Heliyon*, **5**, E02711. https://doi.org/10.1016/j.heliyon.2019.e02711

[13] Katal, R., Zare, H., Rastegar, S.O., Mavaddat, P. and Darzi, G.N. (2014) Removal of Dye and Chemical Oxygen Demand (COD) Reduction from Textile Industrial Wastewater Using Hybrid Bioreactors. *Environmental Engineering and Management Journal*, **13**, 43-50. https://doi.org/10.30638/eemj.2014.007

[14] Yuan, H., Chen, L., Cao, Z. and Hong, F.F. (2020) Enhanced Decolourization Efficiency of Textile Dye Reactive Blue 19 in a Horizontal Rotating Reactor Using Strips of BNC-Immobilized Laccase: Optimization of Conditions and Comparison of Decolourization Efficiency. *Biochemical Engineering Journal*, **156**, Article 107501. https://doi.org/10.1016/j.bej.2020.107501

[15] Singh, P.K. and Singh, R.L. (2017) Bio-Removal of Azo Dyes: A Review. *International Journal of Applied Sciences and Biotechnology*, **5**, 108-126. https://doi.org/10.3126/ijasbt.v5i2.16881

[16] Lade, H., Kadam, A., Paul, D. and Govindwar, S. (2015) Sequencial Aerobic Anaerobic. *EXCLI Journal*, **14**, 158-174.

[17] Mathur, A., Dubey, S., Prasad, R. and Singh, R.P. (2023) Mycelial and Secretome Proteomic Dynamics of *L. squarrosulus* AF5 in Azo Dye Degradation. *Journal of Environmental Chemical Engineering*, **11**, Article 109374. https://doi.org/10.1016/j.jece.2023.109374

[18] Kadam, A.A., Kamatkar, J.D., Khandare, R.V., Jadhav, J.P. and Govindwar, S.P. (2013) Solid-State Fermentation: Tool for Bioremediation of Adsorbed Textile Dyestuff on Distillery Industry Waste-Yeast Biomass Using Isolated *Bacillus cereus* Strain EBT1. *Environmental Science and Pollution Research*, **20**, 1009-1020. https://doi.org/10.1007/s11356-012-0929-6

[19] Balapure, K.H., Jain, K., Chattaraj, S., Bhatt, N.S. and Madamwar, D. (2014)

Co-Metabolic Degradation of Diazo Dye-Reactive Blue 160 by Enriched Mixed Cultures BDN. *Journal of Hazardous Materials*, **279**, 85-95. https://doi.org/10.1016/j.jhazmat.2014.06.057

[20] Ben Mbarek, W., Daza, J., Escoda, L., Fiol, N., Pineda, E., Khitouni, M., *et al*. (2023) Removal of Reactive Black 5 Azo Dye from Aqueous Solutions by a Combination of Reduction and Natural Adsorbents Processes. *Metals*, **13**, Article 474. https://doi.org/10.3390/met13030474

[21] Jain, K., Shah, V., Chapla, D. and Madamwar, D. (2012) Decolorization and Degradation of Azo Dye—Reactive Violet 5R by an Acclimatized Indigenous Bacterial Mixed Cultures-SB4 Isolated from Anthropogenic Dye Contaminated Soil. *Journal of Hazardous Materials*, **213-214**, 378-386. https://doi.org/10.1016/j.jhazmat.2012.02.010

[22] Fareed, A., Zaffar, H., Bilal, M., Hussain, J., Jackson, C. and Naqvi, T.A. (2022) Decolorization of Azo Dyes by a Novel Aerobic Bacterial Strain *Bacillus cereus* Strain ROC. *PLOS ONE*, **17**, e0269559. https://doi.org/10.1371/journal.pone.0269559

[23] Kumaravel, V., Bankole, P.O., Jooju, B. and Sadasivam, S.K. (2022) Degradation and Detoxification of Reactive Yellow Dyes by *Scedosporium apiospermum*: A Mycoremedial Approach. *Archives of Microbiology*, **204**, Article No. 324. https://doi.org/10.1007/s00203-022-02947-1

[24] Kurade, M.B., Waghmode, T.R., Khandare, R.V., Jeon, B.H. and Govindwar, S.P. (2016) Biodegradation and Detoxification of Textile Dye Disperse Red 54 by *Brevibacillus laterosporus* and Determination of Its Metabolic Fate. *Journal of Bioscience and Bioengineering*, **121**, 442-449. https://doi.org/10.1016/j.jbiosc.2015.08.014

[25] Parshetti, G., Kalme, S., Saratale, G. and Govindwar, S. (2006) Biodegradation of Malachite Green by *Kocuria rosea* MTCC 1532. *Acta Chimica Slovenica*, **53**, 492-498.

[26] Priac, A., Badot, P.M. and Crini, G. (2017) Treated Wastewater Phytotoxicity Assessment Using *Lactuca sativa*: Focus on Germination and Root Elongation Test Parameters. *Comptes Rendus Biologies*, **340**, 188-194. https://doi.org/10.1016/j.crvi.2017.01.002

[27] Berridge, M.V., Herst, P.M. and Tan, A.S. (2005) Tetrazolium Dyes as Tools in Cell Biology: New Insights into Their Cellular Reduction. *Biotechnology Annual Review*, **11**, 127-152. https://doi.org/10.1016/S1387-2656(05)11004-7

[28] Klemola, K., Pearson, J., Von Wright, A., Liesivuori, J. and Lindström-Seppä, P. (2007) Evaluating the Toxicity of Reactive Dyes and Dyed Fabrics with the Hepa-1 Cytotoxicity Test. *Autex Research Journal*, **7**, 224-230. https://doi.org/10.1515/aut-2007-070307

[29] Masarbo, R.S., Chebet, J., Shrishail, H.C. and Karegoudar, T.B. (2021) Eco-Friendly Degradative Decolourisation and Detoxification of Azo Dye Amido Black 10B by *Bacillus* sp. Strain AK1. *Chemistry and Ecology*, **37**, 668-682. https://doi.org/10.1080/02757540.2021.1951257

[30] Onder, S., Celebi, M., Altikatoglu, M., Hatipoglu, A. and Kuzu, H. (2011) Decolorization of Naphthol Blue Black Using the Horseradish Peroxidase. *Applied Biochemistry and Biotechnology*, **163**, 433-443. https://doi.org/10.1007/s12010-010-9051-8

[31] Troupis, A., Gkika, E., Triantis, T., Hiskia, A. and Papaconstantinou, E. (2007) Photocatalytic Reductive Destruction of Azo Dyes by Polyoxometallates: Naphthol Blue Black. *Journal of Photochemistry and Photobiology A*: *Chemistry*, **188**, 272-278. https://doi.org/10.1016/j.jphotochem.2006.12.022

[32] Lucas, M.S. and Peres, J.A. (2006) Decolorization of the Azo Dye Reactive Black 5

by Fenton and Photo-Fenton Oxidation. *Dyes and Pigments*, **71**, 236-244. https://doi.org/10.1016/j.dyepig.2005.07.007

[33] Wang, X., Cheng, X., Sun, D. and Qi, H. (2008) Biodecolorization and Partial Mineralization of Reactive Black 5 by a Strain of *Rhodopseudomonas palustris*. *Journal of Environmental Sciences*, **20**, 1218-1225. https://doi.org/10.1016/S1001-0742(08)62212-3

[34] Bansal, P. and Sud, D. (2012) Photodegradation of Commercial Dye, CI Reactive Blue 160 Using ZnO Nanopowder: Degradation Pathway and Identification of Intermediates by GC/MS. *Separation and Purification Technology*, **85**, 112-119. https://doi.org/10.1016/j.seppur.2011.09.055

[35] Lade, H.S., Waghmode, T.R., Kadam, A.A. and Govindwar, S.P. (2012) Enhanced Biodegradation and Detoxification of Disperse Azo Dye Rubine GFL and Textile Industry Effluent by Defined Fungal-Bacterial Consortium. *International Biodeterioration and Biodegradation*, **72**, 94-107. https://doi.org/10.1016/j.ibiod.2012.06.001

[36] Bilal, M., Rasheed, T., Iqbal, H.M.N., Hu, H., Wang, W. and Zhang, X. (2018) Toxicological Assessment and UV/TiO_2-Based Induced Degradation Profile of Reactive Black 5 Dye. *Environmental Management*, **61**, 171-180. https://doi.org/10.1007/s00267-017-0948-7

[37] Roat, C., Kadam, A., Patel, T. and Dave, S. (2016) Biodegradation of Diazo Dye, Reactive Blue 160 by Isolate *Microbacterium sp*. B12 Mutant: Identification of Intermediates by LC-MS. *International Journal of Current Microbiology and Applied Sciences*, **5**, 534-547. https://doi.org/10.20546/ijcmas.2016.503.063

[38] Ahmad, R. and Ansari, K. (2021) Comparative Study for Adsorption of Congo Red and Methylene Blue Dye on Chitosan Modified Hybrid Nanocomposite. *Process Biochemistry*, **108**, 90-102. https://doi.org/10.1016/j.procbio.2021.05.013

[39] Ahmad, R. and Ansari, K. (2022) Novel *In-Situ* Fabrication of L-Methionine Functionalized Bionanocomposite for Adsorption of Amido Black 10B Dye. *Process Biochemistry*, **119**, 48-57. https://doi.org/10.1016/j.procbio.2022.05.015

[40] Radulescu-Grad, M.E., Vlase, G., Ilia, G., Andelescu, A., Popa, S. and Lupea, A.-X. (2020) Amido Black 10B Dye Copper Complex-Synthesis, Characterization and Color Analysis. *Revista de Chimie*, **71**, 27-38. https://doi.org/10.37358/RC.20.8.8276

[41] Neoh, C.H., Lam, C.Y., Lim, C.K., Yahya, A., Bay, H.H., Ibrahim, Z., *et al*. (2015) Biodecolorization of Recalcitrant Dye as the Sole Sourceof Nutrition Using *Curvularia clavata* NZ2 and Decolorization Ability of Its Crude Enzymes. *Environmental Science and Pollution Research*, **22**, 11669-11678. https://doi.org/10.1007/s11356-015-4436-4

[42] Adnan, L.A., Sathishkumar, P., Mohd Yusoff, A.R. and Hadibarata, T. (2015) Metabolites Characterisation of Laccase Mediated Reactive Black 5 Biodegradation by Fast Growing Ascomycete Fungus *Trichoderma atroviride* F03. *International Biodeterioration and Biodegradation*, **104**, 274-282. https://doi.org/10.1016/j.ibiod.2015.05.019

[43] Martorell, M.M., Pajot, H.F. and De Figueroa, L.I.C. (2017) Biological Degradation of Reactive Black 5 Dye by Yeast *Trichosporon akiyoshidainum*. *Journal of Environmental Chemical Engineering*, **5**, 5987-5993. https://doi.org/10.1016/j.jece.2017.11.012

[44] Patil, A.V. and Jadhav, J.P. (2013) Evaluation of Phytoremediation Potential of *Tagetes Patula* L. for the Degradation of Textile Dye Reactive Blue 160 and Assessment of the Toxicity of Degraded Metabolites by Cytogenotoxicity. *Chemosphere*, **92**,

225-232. https://doi.org/10.1016/j.chemosphere.2013.01.089

[45] Al-Adilee, K.J., Abass, A.K. and Taher, A.M. (2016) Synthesis of Some Transition Metal Complexes with New Heterocyclic Thiazolyl Azo Dye and Their Uses as Sensitizers in Photo Reactions. *Journal of Molecular Structure*, **1108**, 378-397. https://doi.org/10.1016/j.molstruc.2015.11.038

[46] Khehra, M.S., Saini, H.S., Sharma, D.K., Chadha, B.S. and Chimni, S.S. (2006) Biodegradation of Azo Dye C.I. Acid Red 88 by an Anoxic-Aerobic Sequential Bioreactor. *Dyes and Pigments*, **70**, 1-7. https://doi.org/10.1016/j.dyepig.2004.12.021

[47] Kyhoiesh, H.A.K. and Al-Adilee, K.J. (2021) Synthesis, Spectral Characterization, Antimicrobial Evaluation Studies and Cytotoxic Activity of Some Transition Metal Complexes with Tridentate (N, N, O) Donor Azo Dye Ligand. *Results in Chemistry*, **3**, Article 100245. https://doi.org/10.1016/j.rechem.2021.100245

[48] Dong, Y. and Jang, J.-H. (2011) Novel Coloration of Cotton Fabrics by UV-Induced Phtografting of Reactive Black 5 and Acrylic acid. *Textile Coloration and Finishing*, **23**, 11-20. https://doi.org/10.5764/TCF.2011.23.1.011

[49] Khunjan, U. and Kasikamphaiboon, P. (2021) Green Synthesis of Kaolin-Supported Nanoscale Zero-Valent Iron Using *Ruellia tuberosa* Leaf Extract for Effective Decolorization of Azo Dye Reactive Black 5. *Arabian Journal for Science and Engineering*, **46**, 383-394. https://doi.org/10.1007/s13369-020-04831-w

[50] Yasmeen, M., Nawaz, M.S., Khan, S.J., Ghaffour, N. and Khan, M.Z. (2023) Recovering and Reuse of Textile Dyes from Dyebath Effluent Using Surfactant Driven Forward Osmosis to Achieve Zero Hazardous Chemical Discharge. *Water Research*, **230**, Article 119524. https://doi.org/10.1016/j.watres.2022.119524

[51] Jha, P., Jobby, R. and Desai, N.S. (2016) Remediation of Textile Azo Dye Acid Red 114 by Hairy Roots of *Ipomoeacarnea Jacq*. and Assessment of Degraded Dye Toxicity with Human Keratinocyte Cell Line. *Journal of Hazardous Materials*, **311**, 158-167. https://doi.org/10.1016/j.jhazmat.2016.02.058

[52] Little, M.C., Gawkrodger, D.J. and Macneil, S. (1996) Chromium-and Nickel-Induced Cytotoxicity in Normal and Transformed Human Keratinocytes: An Investigation of Pharmacological Approaches to the Prevention of Cr(VI)-Induced Cytotoxicity. *British Journal of Dermatology*, **134**, 199-207. https://doi.org/10.1111/j.1365-2133.1996.tb07602.x